11. Diaz, J. M.; Caballero, M.; Atonio, *J. Analyst* **1990**, *115*, 1201.
12. Hagadone, M.; Zeitlin, H. *Anal. Chim. Acta* **1976**, *86*, 289.
13. Hiraide, M.; Mizuike, A. *Japan Analyst* **1974**, *23*, 522.
14. Mizuike, A.; Fukuda, K.; Suzuki, S. *Japan Analyst* **1969**, *18*, 519.
15. Kim, Y. S.; Han, J. S.; Choi, H. S. *Anal. Sci.* **1991**, *7*(Supplement), 1347.
16. Aoyama, M.; Hobo, T.; Suzuki, S. *Anal. Chim. Acta* **1981**, *129*, 237.
17. Berg, E. W.; Downey, A. *Anal. Chim. Acta* **1980**, *120*, 237.
18. Sung, W. S; Choi, H. S.; Kim, Y. S. *J. Korean Chem. Soc.* **1993**, *37*(3), 327.
19. Kim, Y. S.; Park, S. J.; Choi, J. M. *Bull. Korean Chem. Soc.* **1993**, *14*(3), 330.
20. Cho, M. S.; Lim, H.; Kim, Y. S. *J. Korean Chem. Soc.* **1994**, *38*(9), 667.
21. Kim, Y. S.; Kim, K. C. *Bull. Korean Chem. Soc.* **1995**, *16*(7), 582.
22. Jeon, M. K.; Choi, J. M.; Kim, Y. S. *Anal. Sci. & Tech.* **1996**, *9*(4), 336.
23. Kotsuji, K.; Kaneyama, Y.; Arikawa, M.; Hayashi, S. *Talanta* **1977**, *26*, 475.
24. Kotsuji, K.; Kimura, I.; Yoshimura, H. *Talanta* **1979**, *28*, 263.
25. Caragay, A. B.; Karger, B. L. *Anal. Chem.* **1966**, *38*, 652.
26. Elhanan, J.; Karger, B. L. *Anal. Chem.* **1969**, *41*, 671.
27. Cervera, J.; Cela, R. *Anal. Chim. Acta* **1982**, *107*, 1425.
28. Kiwan, A. M.; Kassim, A. Y. *Anal. Chim. Acta.* **1977**, *88*, 177.
29. Fisher, H. *Angew. Chem.* **1934**, *47*, 685.
30. Akaiwa, H.; Kawamoto, H.; Tanaka, T. *Anal. Sci.* **1987**, *3*, 113.
31. Aoyama, M.; Hobo, T.; Suzuki, S. *Anal. Chim. Acta.* **1982**, *141*, 427.
32. Nakashima, S. *Anal. Chem.* **1979**, *51*, 654.
33. Hiraide, A.; Mizuike, A. *Talanta* **1975**, *22*, 539.

Laser-Induced Fluorescence Spectroscopy of the S_1-S_0 ($^1B_2$-$^1A_1$) Transition of Dimethyldiazirine

Taek-Soo Kim, Sang Kyu Kim, Young S. Choi*, and Ilhwan Kwak†

Department of Chemistry, Inha University, Incheon 402-751, Korea
†Bolak Company Limited, Technical Research Institute, Hwasung-gun, Kyungki-do, Republic of Korea
Received April 17, 1998

The fluorescence excitation (FE) spectrum of the S_1-S_0 ($^1B_2$-$^1A_1$) transition of dimethyldiazirine cooled in supersonic jet expansions has been obtained. Dispersed fluorescence (DF) spectra have also been taken for some prominent features of the FE spectrum. Vibrational analyses of the FE and DF spectra with the help of an *ab initio* molecular orbital calculation lead to some new vibrational assignments and refined fundamental frequencies.

Introduction

Diazirines are unique in that they contain a highly strained, three-membered, heterocyclic CN_2 ring. Since these molecules have a strong absorption band in the near ultraviolet (UV) region, they have been the topics of many photochemical and spectroscopic studies since the three-membered ring structure was first established.[1] Diazirines decompose into a carbene radical and an N_2 molecule when photolyzed in the ultraviolet (UV) wavelength.[2,3] While the infrared spectrum of diazirine was first analyzed by Ettinger,[4] most of the early spectroscopic studies on diazirine and substituted diazirines have been performed by Merritt and coworkers.[5-13] They determined the structures of methyl- and dimethyldiazirines with microwave spectroscopy[10,11] and analyzed the infrared spectra of diazirine and methyldiazirines, confirming the cyclic strucuture.[12,13] Robertson and Merritt have reported the electronic spectra for the n-π^* transition of various diazirines.[6-9] For diazirine, the simplest member of the group, the strongest band system in UV was assigned to the $\tilde{A}^1B_1$-X^1A_1 transition and the band origin was determined to be located at 31,187 cm^{-1}.[6] A long progression of the C-N symmetric stretching vibration (ν_3) has been observed. Substituted diazirines such as methyl-, dimethyl, bromomethyl-, and chloromethyldiazirines show similar spectra to the unsubstituted counterpart except that the transition frequencies exhibit a significant red shift upon substitution.[7-9] The electronic spectroscopy of difluorodiazirine was first investigated by Lombardi *et al.*[14] and later by Hepburn and Hollas.[15] Vandersall and Rice have provided the fluorescence spectra from single vibronic levels and investigated the collisional relaxation in the $^1B_1$(n-π^*) electronic manifold.[16] More recently Neusser and coworkers have obtained and analyzed the high-resolution Doppler-free two-photon spectrum providing a more refined excited state geometry and more fundamental frequencies.[17]

*Author to whom correspondence should be addressed.

Recently, fluorescence from the $^1(n\pi^*)$ state of several alkyldiazirines has been observed both in solution[18,19] and in the gas phase.[20] The fluorescence provides a simple and sensitive tool of laser-induced fluorescence for electronic spectroscopy, which enables one to obtain rotationally and vibrationally cold spectra of diazirines in supersonic jet expansions. The spectra of molecules cooled in jet expansions make the vibrational analysis simple and dispose of possible complications due to hot band transitions. By taking advantage of the fluorescence, we have initiated a series of studies on the spectroscopy and photodissociation dynamics of various diazirines in the gas phase. Recently we have reported the fluorescence excitation (FE) and photoacoustic spectra of 3,3'-dimethyldiazirine (DMD) in the gas phase.[20] The energy dependence of the band intensity of two spectra indicated that two radiationless decay channels, vibrational predissociation and internal conversion, are mainly responsible for the decay of the DMD in their first excited singlet (S_1) state in the gas phase.

DMD has C_{2v} symmetry and its ground state structure has been determined by microwave spectroscopy.[10]

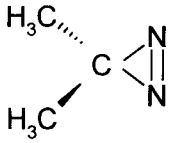

To our knowledge, the absorption spectrum, which was reported by Robertson and Merritt, is the only available spectroscopic data on the electronic transitions of DMD.[9] They reported that the origin of the allowed $^1B_2(n\pi^*)$-$^1A_1$ system is located at 27,923 cm^{-1} and a weak system occurs 126 cm^{-1} red from the singlet-singlet system. The weak system was assigned to the triplet-singlet $\pi^*\leftarrow\pi$ transition, which was recently reassigned to a hot band of the allowed $^1B_2(n\pi^*)$-$^1A_1$ system.[21] They also analyzed the vibrational structure of the $^1B_2(n\pi^*)$-$^1A_1$ system and determined the fundamental frequencies of the $^1B_2(S_1)$ state with the help of IR data.

In this paper, we report the results of the spectroscopic study on the S_1-S_0 transition of DMD by using laser-induced fluorescence and supersonic jet expansions. An *ab initio* calculation is performed to help in assigning the vibrational frequencies observed in the dispersed fluorescence (DF) spectra. Some new vibrational assignments and refined values of the fundamental frequencies are reported.

Experimental

A schematic of the experimental setup employed in this work is shown in Figure 1. The supersonic jet apparatus consists of a vacuum chamber, a pulsed valve, and an oil diffusion pump backed with a mechanical pump. The vacuum chamber is basically a 20 cm diameter stainless steel 6-way cross. On the top flange, the pulsed valve (General Valve) was placed facing downward so that the jet was directed into the pumping system. Two 50 cm long side-arms, through which the excitation laser beam passes, are horizontally attached to the chamber. Several irises were placed inside the arms to reduce the scattered light. One of two flanges, parallel to the plane consisting of the laser

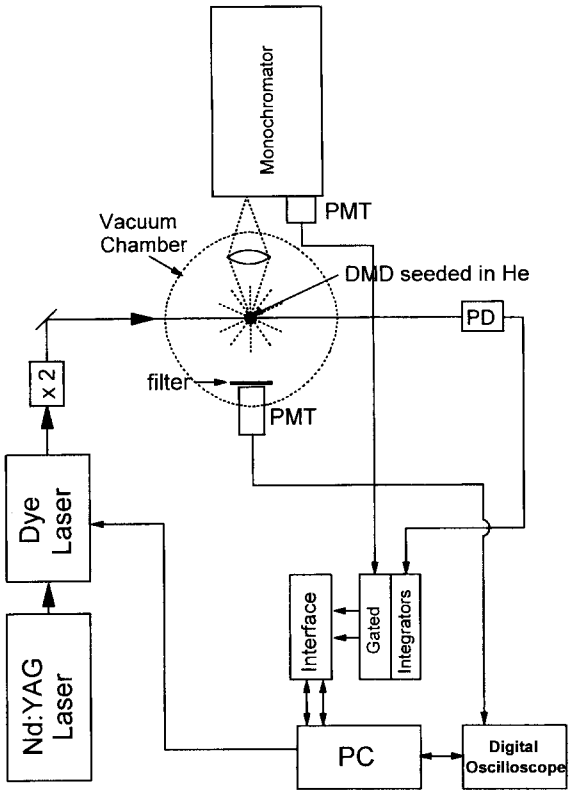

Figure 1. Schematic of the experimental setup. PMT-photomultiplier tube, PD-photodiode, PC-personal computer.

beam and the jet axis, was machined to hold a 50 mm diameter photomultiplier tube (PMT). The chamber was evacuated with a 20 cm oil diffusion pump (Varian VHS-6) with a liquid N_2 baffle on it and a mechanical pump with a nominal pumping speed of 600 L/min. The base pressure was below 1×10^{-6} Torr without the nozzle operation and 2×10^{-5} Torr with the nozzle on.

About 3% premixtures of dimethyldiazirine in He were prepared in a stainless steel cylinder of the internal volume of 4 liters at least 12 hrs prior to each experiment. The mixture, kept at the pressure of 1 atm, was expanded through a 0.5 mm diameter nozzle which was driven with a home-made driver.

The output beam from a pulsed dye laser (Lambda Physik SCANmate 2E) pumped with a Q-switched Nd: YAG laser (Spectra-Physics GCR-150) was frequency-doubled in a KDP crystal. The phase-matching angle of the crystal was set by an autotracker (Inrad I) controlled by a personal computer. The second harmonic output, which was separated from the fundamental with three dichroic mirrors was directed through the side arms, exciting the cooled DMD molecules in the jet expansions. The distance from the nozzle to the excitation laser beam was set 25 mm. Fluorescence from the excited DMD was collected with a 50 mm diameter f/2 quartz lens, filtered with a color filter (Schott GG-380) and a slit aperture, and then detected with a PMT (Hamamastu H1161). The PMT output signal was integrated in a gated integrator (SRS 250) and stored in the PC with the corresponding laser wavelength. When DF spectrum was taken, the interaction region was imaged onto the input slit of a scanning monochromator with a 1200

grooves/mm grating blazed at 300 nm. The focal length of the monochromator is 45 cm and the spectral resolution with 0.5 mm wide slits was ~1 nm. The shot-to-shot fluctuation of the excitation laser pulses was monitored with a pyroelectric joulemeter (Molectron P5-01). The energy of the excitation pulse was kept at ≤ 1.0 mJ/pulse and the laser beam was unfocused to avoid saturation of transitions. The optogalvanic spectrum of a Ne hollow cathode lamp provided a frequency calibration for the dye laser with an accuracy of ± 0.2 cm^{-1}.

The DMD sample was synthesized following the procedure described previously.[22]

Since DMD has 27 vibrational modes and the assignment has not been completed, *ab initio* calculations on the S_0 state were performed to help in the assignment of the DF spectra. The calculations were executed with a personal computer equipped with an Intel Pentium 120 MHz processor and 32MB RAM and by the standard methods included in the Gaussian 94 for Windows package.[23] The geometry optimization and vibrational frequency calculations were performed at the HF and MP2 levels and the 6-31G(d) basis set was employed in all calculations. Fundamental frequencies of the a_1 modes, obtained in the MP2/6-31G(d) calculation, are listed in Table 3.

Results and Discussion

The jet-cooled FE spectrum of DMD is obtained for the first time and shown in Figure 2. As expected from the low rotational temperature of the jet expansions, each vibronic band represents a sharp peak, facilitating accurate determination of the band positions. The frequencies and relative intensities of the prominent features are summarized in Table 1.

The S_1-S_0 transition of DMD was first investigated by Robertson and Merritt and assigned to the $^1B_2(n\pi^*)\leftarrow{}^1A_1$ system, based on the rotational structures of the vibronic bands.[9] The positions of the vibronic bands of our jet spectrum are in a good agreement with those reported by Robertson and Merritt,[9] confirming that it is the $S_1\leftrightarrow S_0$ ($^1B_2\leftrightarrow 1A_1$) transition that carries the FE and DF spectra obtained in this work. As observed in the FE spectrum at room temperature,[20] the band intensity rapidly decreases with increasing energy, and thus no band has a noticeable intensity above 1500 cm^{-1}. This drastic decrease of band intensity was attributed to predissociation over a small barrier of *ca.* 300 cm^{-1} on the S_1 potential energy surface.[20]

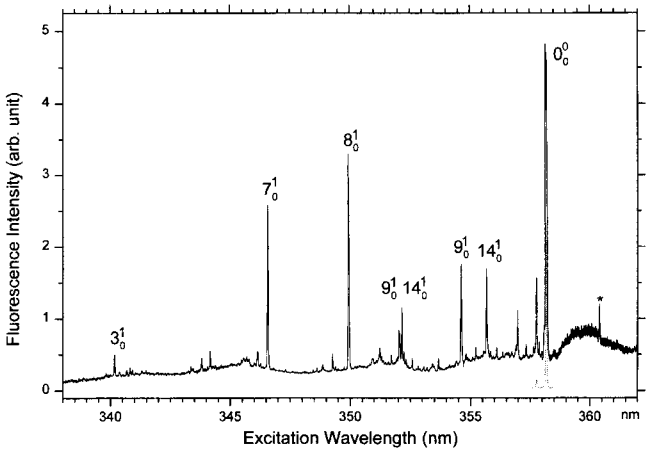

Figure 2. Fluorescence excitation spectrum for the $S_1\leftarrow S_0$ ($^1B_2\leftarrow{}^1A_1$) transition of dimethyldiazirine in supersonic free jet expansions. The origin band is broken since the whole spectrum was obtained at a higher sensitivity in order to enhance the weak bands. A short scan taken at a lower sensitivity is shown near the origin band with a broken line. The peak marked with a * is from impurity. The broad feature at the red side of the origin band is due to the van der Waals clusters of DMD with He atoms.

Table 1. Assignment of bands observed in the fluorescence excitation spectrum of 3,3'-dimethyldiazirine

Transition frequency	Vibrational Energy	Relative intensity	Assignment
27746.5	-172.8	24	impurity
27919.4	0.0	1000	0^0_0
27942.2	22.9	8	
27951.0	31.6	48	
27984.8	65.4	8	
28012.7	93.4	31	
28018.5	99.2	Shoulder	
28082.2	162.8	7	
28115.7	196.3	55	14^2
28199.5	280.2	61	9^1
28396.5	477.2	34	9^114^2
28405.5	486.2	19	
28470.5	551.1	8	
28576.3	656.9	130	8^1
28630.6	711.3	11	
28853.7	934.4	100	7^1
28889.2	969.9	10	
29055.8	1136.5	11	7^114^2
29086.1	1166.8	8	6^1
29341.2	1421.9	5	4^1
29396.8	1477.5	15	3^1

Figures 3 and 4 show the DF spectra for the major bands observed in the FE spectrum. The vibronic bands observed

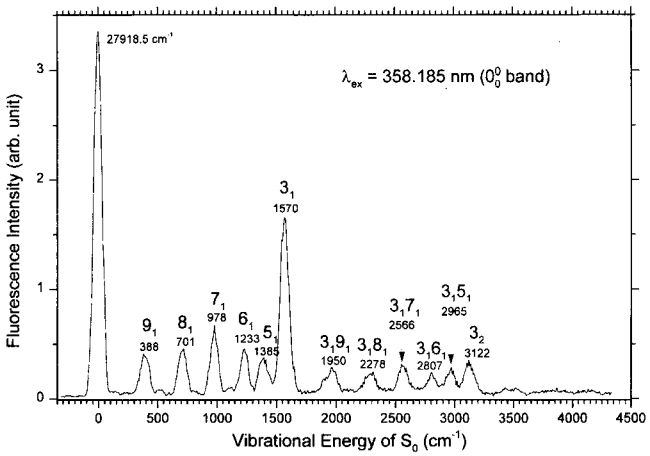

Figure 3. Dispersed fluorescence spectrum from the origin of the S_1 state. The band assignments and frequencies are given on top of the prominent peaks.

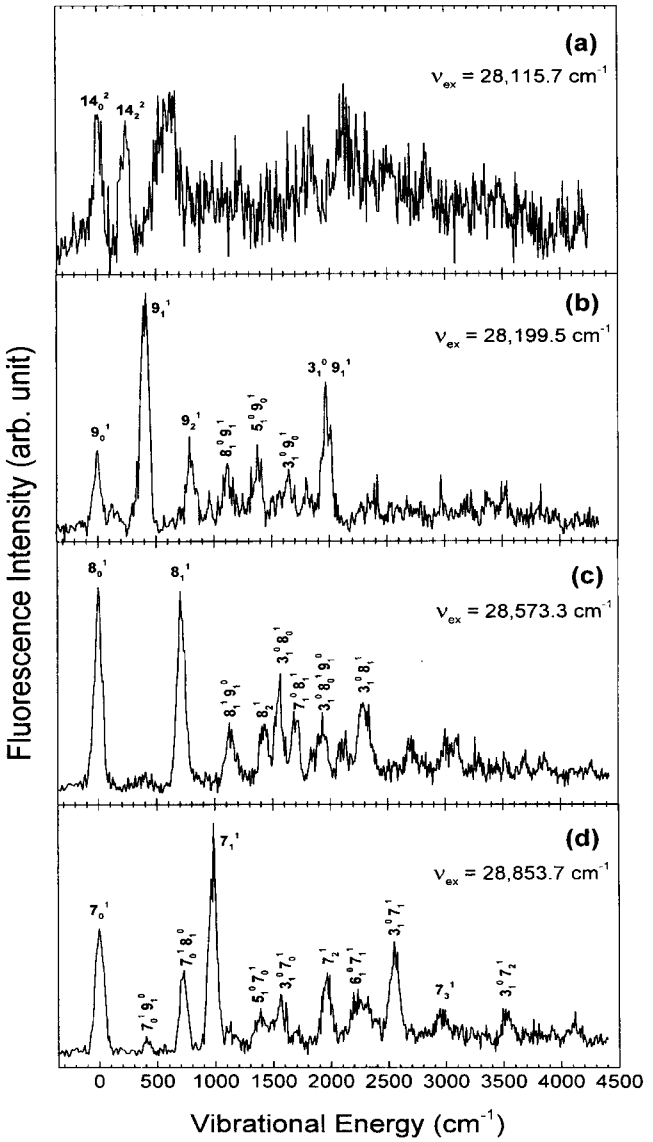

Figure 4. Dispersed fluorescence spectra from (a) the 14_0^2 band, (b) the 9_0^1 band, (c) the 8_0^1 band, and (d) the 9_0^1 band. Due to the low S/N ratio of the spectra, the uncertainty of peak position measurements is about $\pm$0.2 nm.

in the DF spectrum from the origin band are summarized with their assignment in Table 2. Since fluorescence quantum yields of the S_1 levels are fairly low, it was not feasible to obtain the emission spectra with a reasonably high signal-to-noise ratio except from the origin band. Analysis of each DF spectrum is discussed below with the assignment of the upper level.

Vibrational Analysis

The drastic decrease of band intensities with increasing vibrational energy not only limits the spectrum less than 1500 cm^{-1} above the origin, but also prevents us from observing some long progressions which would help assignment. The DF spectra, which are assigned with the help of the IR spectrum[12] and the *ab initio* frequencies, were extremely useful for analyzing the vibrational features of the S_1 state. Assignments of strong features are straightforward, and mostly agree with those of Robertson and Merritt.[9] Assignment of the weak bands in the FE spectrum, however, is non-trivial since a high signal-to-noise DF spectrum was not obtainable. Hence assignment of the weak features was not established by dispersed fluorescence spectra, but was based solely on combinations of the S_1 frequencies obtained from the relatively strong bands. All of the vibronic bands observed in the FE spectrum are summarized in Table 1 with their assignments.

Table 2. Transitions observed in the dispersed fluorescence spectrum of 3,3'-dimethyldiazirine excited to the origin (0^0) level

Position[a]/cm^{-1}	Relative Intensity	Assignment
0	100	0_0^0
-395	14	9_1^0
-714	15	8_1^0
-982	18	7_1^0
-1235	14	6_1^0
-1396	13	5_1^0
-1573	54	3_1^0
-1961	13	$3_1^0 9_1^0$
-2293	11	$3_1^0 8_1^0$
-2569	12	$3_1^0 7_1^0$
-2812	8	$3_1^0 6_1^0$
-2972	10	$3_1^0 5_1^0$
-3129	14	3_2^0

[a] Band positions are given relative to the 0_0^0 band at 27,919.4 cm^{-1}.

Origin (0_0^0) Band. Identification of the origin band is trivial in the jet spectrum, as shown in Figure 2. The origin of the S_1 state is determined to be located at 27,919.4 cm^{-1}, which is in reasonable agreement with the value of 27,923 cm^{-1} reported by Robertson and Merritt.[9]

The emission spectrum from the 0^0 level is illustrated in Figure 3. The major bands, which are mostly the progressions and combinations involving the a_1 modes, are listed with assignments in Table 2. As expected from the absorption spectrum,[9] the progression of the N=N stretching (ν_3) mode is most noticeable. The fundamentals of the totally symmetric ν_5, ν_6, ν_7, ν_8, and ν_9 appear built on the ν_3 progression.

$0^0 + 196$ cm^{-1}. This band, observed 196 cm^{-1} above the origin, was not reported by Robertson and Merritt,[9]

Table 3. Fundamental frequencies of the S_0 and S_1 states of 3,3'-dimethyldiazirine

	$\nu(S_0)$/cm^{-1}			$\nu(S_1)$/cm^{-1}
mode (symmetry)	*Ab initio* MP2/6-31G	from DF spectra	From IR spectrum[c]	from FE spectrum
ν_3 (a_1)	1,480	1,565	1,603.3	1,477.5
ν_4 (a_1)	1,435	-	1,458	1,421.9?
ν_5 (a_1)	1,384	1,389	1,391.1	-
ν_6 (a_1)	1,209	1,235	1,136	1,166.8?
ν_7 (a_1)	968	979	993	934.4
ν_8 (a_1)	697	716	-	656.9
ν_9 (a_1)	340	405/405.9[b]	433	280.2
ν_{14} (a_2)	131	123.5	-	98.2

[a] multiplied by a scaling factor of 0.94.[25-27] [b] from a hot band in the FE spectrum (reference 21). [c] from the infrared spectrum of Reference 12.

presumably because of its weak intensity. In the FE spectrum, it appears relatively strong since the level is located below the barrier for predissociation.[20] Although emission from this level is very weak and its DF spectrum (Figure 4(a)) reveals a poor S/N ratio, a 247 cm^{-1} red band from the resonance band is identifiable. Since there is no a_1 mode with the frequency of 247 cm^{-1} in DMD, it is supposed to be an overtone of a non-totally symmetric vibration. Such a low-frequency vibration has never been experimentally observed in DMD, and thus we referred to the *ab initio* frequencies. Since the *ab initio* calculation shows that the ν_{14} has the a_2 symmetry and 131 cm^{-1} of frequency in the ground electronic state, the 196 cm^{-1} band in the FE spectrum is tentatively assigned to the 14_0^2 transition. Then the 247 cm^{-1} band in the DF spectrum is assigned to the 14_2^2. Although discrepancy between the measured and calculated frequencies is non-negligible, it is acceptable considering the low resolution and poor signal-to-noise ratio of the DF spectrum.

$0^0 + 280.2$ cm^{-1}. This band was observed at 278 cm^{-1} by Robertson and Merritt, but was left unassigned. The DF spectrum from this level, given in Figure 4(b), shows a strongly enhanced line at 406 cm^{-1} red from the resonance band, compared with the relative band intensity distribution of the DF spectrum from the origin band. Since this frequency is close to 433 cm^{-1} of the ν_9 (CCC deformation) measured in the infrared spectrocopy,[12] we assign this feature to the 9_0^1 band.

$0^0 + 477.2$ cm^{-1} and $0^0 + 486.2$ cm^{-1}. Since the $0^0 + 477.2$ cm^{-1} and $0^0 + 486.2$ cm^{-1} bands are in close proximity, it is not easy to unambiguously assign these bands. Even worse is that the bands are too weak for us to obtain the corresponding DF spectra. In the absorption spectrum,[9] these two bands were not resolved and thus the whole feature was assigned to the 9_0^1 band. As discussed above, however, it is more reasonable to be assign the 280.2 cm^{-1} band to the 9_0^1 band. We tentatively assign the 477.2 cm^{-1} feature to the $9^1 14^2$ based upon a combination of the known frequencies of the ν_9 and ν_{14} in S_1, but the 486.2 cm^{-1} band is left unassigned.

$0^0 + 656.9$ cm^{-1}. This band is the second strongest feature in the FE spectrum and thus gives a relatively strong emission. The DF spectrum is shown in Figure 4(c). A strong 714 cm^{-1} red band from the resonance band must be the fundamental of the ν_8 of S_0, which was reported to be 738 cm^{-1} in IR spectroscopy, and thus the upper level of the S_1 is assigned to the 8^1, in agreement with that reported by Robertson and Merritt.

$0^0 + 934.4$ cm^{-1}. The DF spectrum from this level is illustrated in Figure 4(d). The strongest band at 985 cm^{-1} is assigned to the fundamental of the ν_7 (CH_3 rock) of S_0, the frequency of which is reported to be 987.6 cm^{-1} by IR spectroscopy. Hence the 934.4 cm^{-1} feature in the FE spectrum is assigned to the 7_0^1 band, which is also in agreement with that reported by Robertson and Merritt.

$0^0 + 1477.5$ cm^{-1}. Although this band is quite weak, it is straightforward to assign it to the 3_0^1 band since it is the only strong line near the wavelength where the 3_0^1 band is expected. The absorption[24] and photoacoustic spectra[20] confirm the fact.

Other weak bands. It is more difficult to assign these weak features than the strong ones because DF spectrum is not obtainable for them. Some are tentatively assigned based on the combination of frequencies but most of them are left unassigned. The 477.2 cm^{-1} and 1136.5 cm^{-1} features are assigned to the $9_0^1 14_0^2$ and $7_0^1 14_0^2$ bands, respectively, based upon combinations of the known frequencies. A tentative assignment of the two bands observed at 1166.8 cm^{-1}, and 1421.9 cm^{-1} to the 6_0^1 and 4_0^1 bands, respectively, is provided referring to the corresponding *ab initio* frequencies in S_0. We believe that some of the weak transition lines, in particular the ones observed at the vibrational energy below *ca.* 100 cm^{-1}, are involved with hindered motions of two methyl groups, but detailed analysis is not attempted in this work.

Summary

The FE spectrum of the S_1-S_0 ($^1B_2$-$^1A_1$) transition of DMD, cooled in supersonic jet expansions, provided a well-resolved picture of the vibronic levels of the S_1 state, although the accessible frequency range was seriously limited below 1500 cm^{-1} due to rapid predissociation. *Ab initio* frequencies were employed to assign the low-frequency modes whose frequencies were not reported in the IR spectroscopy. The FE spectrum as well as the DF spectra from the major features enabled us to reassign some bands whose previous assignments were ambiguous.

Acknowledgment. This work was supported by the Ministry of Education of Korea through the 1996-1997 Basic Science Research Institute Program (Project No. BSRI-96-3432) and the Korean Science and Engineering Foundation (Project No. 95-0501-04-01-3). Authors at Inha University acknowledge the support of the 1997 Inha University Research Fund.

References

1. Pierce, L.; Dobyns, V. J. *J. Am. Chem. Soc.* **1962**, *84*, 2651.
2. Frey, H. M. *Adv. Photochem.* **1966**, *4*, 225. and references cited therein.
3. Liu, M. T. H. *Chem. Soc. Rev.* **1982**, *11*, 136. and references cited therein.
4. Ettinger, R. *J. Chem. Phys.* **1964**, *40*, 1693.
5. Merritt, J. A. *Can. J. Phys.* **1962**, *40*, 1683.
6. Robertson, L. C.; Merritt, J. A. *J. Mol. Spectrosc.* **1966**, *19*, 372.
7. Robertson, L. C.; Merritt, J. A. *J. Mol. Spectrosc.* **1967**, *24*, 44.
8. Robertson, L. C.; Merritt, J. A. *J. Chem Phys.* **1972**, *57*, 941.
9. Robertson, L. C.; Merritt, J. A. *J. Chem. Phys.* **1972**, *56*, 2919.
10. Wollrab, J. E.; Scharpen, L. H.; Ames, D. P.; Merritt, J. A. *J. Chem. Phys.* **1968**, *49*, 2405.
11. Wollrab, J. E.; Scharpen, L. H.; Ames, D. P.; Merritt, J. A. *J. Chem. Phys.* **1969**, *50*, 2063.
12. Mitchell, R. W.; Merritt, J. A. *J. Mol. Spectrosc.* **1968**, *27*, 197.
13. Mitchell, R. W.; Merritt, J. A. *J. Mol. Spectrosc.* **1969**, *29*, 174.

14. Lombardi, J. R.; Klemperer, W.; Robin, M. B.; Basch, H.; Kuebler, N. A. *J. Chem. Phys.* **1969**, *51*, 33.
15. Hepburn, P. H.; Hollas, J. M. *J. Mol. Spectrosc.* **1974**, *50*, 126.
16. Vandersall, M.; Rice, S. A. *J. Chem. Phys.* **1983**, *79*, 4845.
17. (a) Sieber, H.; Riedle, E.; Neusser, H. *J. Chem. Phys. Lett.* **1990**, *169*, 191. (b) Sieber, H.; Bruno, A. E.; Neusser, H. J. *J. Phys. Chem.* **1990**, *94*, 203.
18. Modarelli, D. A.; Morgan, S.; Platz, M. S. *J. Am. Chem. Soc.* **1992**, *114*, 7034.
19. Modarelli, D. A.; Platz, M. S. *J. Am. Chem. Soc.* **1993**, *115*, 470.
20. Kim, T.-S.; Choi, Y. S.; Kwak, I. *J. Photochem. Photobiol. A.* **1997**, *108*, 123.
21. Kim, T.-S.; Kim, S. K.; Choi, Y. S.; Kwak, I. *J. Chem. Phys.* **1997**, *107*, 8719.
22. Schmitz, E.; Ohme, R. *Chem. Ber.* **1961**, *94*, 2166.
23. Frisch, M. J.; Trucks, G. W.; Schlegel, H. B.; Gill, P. M. W.; Johnson, B. G.; Robb, M. A.; Cheeseman, J. R.; Keith, T. A.; Petersson, G. A.; Montgomery, J. A.; Raghvachari, K.; Al-Laham, M. A.; Zakrzewski, V. G.; Oritiz, J. V.; Foresman, J. B.; Cioslowski, J.; Stefanov, B. B.; Nanayakkara, A.; Challacombe, M.; Peng, C. Y.; Ayala, P. Y.; Chen, W.; Wong, M. W.; Andres, J. L.; Replogle, E. S.; Gomperts, R.; Martin, R. L.; Fox, D. J.; Binkley, J. S.; Defrees, D. J.; Baker, J.; Stewart, J. P.; Head-Gordon, M.; Gonzalez, C.; Pople, J. A. *Gaussian 94*, Gaussian, Inc., Pittsburgh, PA, 1995.
24. Kim, T.-S.; Choi, Y. S. a low-resolution absorption spectrum of the gaseous dimethyldiazirine obtained with a UV-visible spectrometer, unpublished result.
25. Hout, R. F.; Levi, B. A.; Hehre, W. J. *J. Comput. Chem.* **1982**, *3*, 234.
26. Defrees, D. J.; McLean, A. D. *J. Chem. Phys.* **1985**, *82*, 333.
27. Pople, J. A.; Scott, A. P.; Wong, M. W.; Radom, L. *Isr. J. Chem.* **1993**, *33*, 345.

Molecular Dynamics Simulation for Bilayers of Alkyl Thiol Molecules at Solid-Solid Interfaces

Song Hi Lee*, Han Soo Kim†, and Hyungsuk Pak‡

Department of Chemistry, Kyungsung University, Pusan 608-736, Korea
†Department of Industrial Chemistry, Kangnung National University, Kangnung 212-702, Korea
‡Department of Chemistry, Seoul National University, Seoul 151-740, Korea
Received May 1, 1998

We present the results of molecular dynamics simulations for three different systems of bilayers of long-chain alkyl thiol [$S(CH_2)_{15}CH_3$] molecules on an solid-solid interface using the extended collapsed atom model for the chain-molecule. It is found that there exist two possible transitions: a continuous transition characterized by a change in molecular interaction between sites of different chain molecules with increasing area per molecule and a sudden transition from an ordered lattice-like state to a liquid-like state due to the lack of interactions between sites of chain molecules on different surfaces with increasing distance between two solid surfaces. The third system displays a smooth change in probability distribution characterized by the increment of *gauche* structure in the near-tail part of the chain with increasing area per molecule. The analyses of energetic results and chain conformation results demonstrate the characteristic change of chain structure of each system.

Introduction

In a previous paper,[1] we have performed several molecular dynamics (MD) simulations of monolayers of long-chain alkyl thiol[$S(CH_2)_{15}CH_3$] molecules on an air-solid interface using an extended collapsed atom model for the chain-molecule and a gold surface for the solid surface. We investigated the structure and thermodynamics of monolayers of long-chain alkyl thiol molecules on an air-solid interface as a function of area per molecule, especially, to study the phase transition in the monolayer, the fraction of trans formation, the thickness of the monolayer, monolayer tilting,Slattice defects, and diffusion of the chain-molecules. Also additional studies of how the area per molecule of the chain-molecule on the surface affects the characterization of Langmuir monolayer were carried out. The results from our MD simulations showed three possible transitions: a continuous transition characterized by a change in molecular configuration without changing in the lattice structure, a sudden transition characterized by the distinct lattice defects and perfect islands, and a third transition characterized by the appearance of a random, liquid-like state.

We have extended this study[1] to the bilayers of alkyl thiol molecules at a solid-solid interface. The bilayer of chain-molecules is very important for biological membranes,[2] because, in the bilayers, lipid-lipid interactions as well as lipid-intrinsic molecule (e.g., cholesterol and protein) interactions may be studied for a reasonably well-defined system. Also this study helps to understand the system of